Dose distribution as outcome predictor for Gamma Knife radiosurgery on vestibular schwannoma

P. P. J. Langenhuizen, H. van Gorp, S. Zinger, H. B. Verheul, S. Leenstra, et al.

P. P. J. H. Langenhuizen, H. van Gorp, S. Zinger, H. B. Verheul, S. Leenstra, P. H. N. de With, "Dose distribution as outcome predictor for Gamma Knife radiosurgery on vestibular schwannoma," Proc. SPIE 10950, Medical Imaging 2019: Computer-Aided Diagnosis, 109504C (13 March 2019); doi: 10.1117/12.2512472

SPIE.

Event: SPIE Medical Imaging, 2019, San Diego, California, United States

Dose distribution as outcome predictor for Gamma Knife radiosurgery on vestibular schwannoma

P.P.J.H. Langenhuizen[a,b], H. van Gorp[a], S. Zinger[a], H.B. Verheul[b], S. Leenstra[b], and P.H.N. de With[a]

[a]Eindhoven University of Technology, De Zaale, Eindhoven, the Netherlands
[b]Elisabeth-TweeSteden Hospital, Hilvarenbeekseweg 60, Tilburg, the Netherlands

ABSTRACT

Vestibular schwannomas are benign brain tumors that can be treated radiosurgically with the Gamma Knife in order to stop tumor progression. However, in some cases tumor progression is not stopped and treatment is deemed a failure. At present, the reason for these failed treatments is unknown. Clinical factors and MRI characteristics have been considered as prognostic factors. Another confounder in the success of treatment is the treatment planning itself. It is thought to be very uniformly planned, even though dose distributions among treatment plans are highly inhomogeneous. This paper explores the predictive value of these dose distributions for the treatment outcome. We compute homogeneity indices (HI) and three-dimensional histogram-of-oriented gradients (3D-HOG) and employ support vector machine (SVM) paired with principal component analysis (PCA) for classification. In a clinical dataset, consisting of 20 tumors that showed treatment failure and 20 tumors showing treatment success, we discover that the correlation of the HI values with the treatment outcome presents no statistical evidence of an association (52.5% accuracy employing linear SVM and no statistical significant difference with t-tests), whereas the 3D-HOG features concerning the dose distribution do present correlations to the treatment outcome, suggesting the influence of the treatment on the outcome itself (77.5% accuracy employing linear SVM and PCA). These findings can provide a basis for refining towards personalized treatments and prediction of treatment efficiency. However, larger datasets are needed for more extensive analysis.

Keywords: Gamma Knife radiosurgery, vestibular schwannoma, dose distribution, homogeneity index, three-dimensional histogram of oriented gradients, PCA, classification, SVM, outcome prediction.

1. INTRODUCTION

The selection of the optimal treatment strategy for a specific brain tumor is often based on a combination of (1) the personal experience of the treating physician, (2) the obtained clinical results in the field of brain tumor treatment with respect to the different strategies, and (3) quality-of-life surveys of the diagnosed patients. Moreover, the dependence on the first point can be further detailed, as also the treatment goal of the physician plays a role. More specifically, the treatment goal can be either cure-oriented or tumor-control oriented, along with maintenance of the neurologic function and preserving quality of life (QOL).[1] Specifically, for vestibular schwannomas (VS) the discussion is ongoing whether these tumors should be treated microsurgically or radiosurgically, or should be monitored and only treated when tumor progression is observed. These benign brain tumors of the eighth cranial nerve progress slowly or even remain quiescent for many years. So, if the treatment goal is to obtain tumor control, it would make sense to only treat the VS tumor when progression is observed. Furthermore, QOL surveys show that patients demonstrate significantly higher QOL scores when their VS is only monitored, compared to patients that underwent radiosurgery or microsurgery.[2] However, there are medical teams that advocate early radiosurgical intervention, as it obtains higher rates of hearing preservation.[3]

Even if active treatment is advised, there is no clear scientific consensus on which treatment option should be preferred. However, non-randomized control trials show an advantage for radiosurgery, specifically Gamma Knife radiosurgery (GKRS), over microsurgery in sporadic VS smaller than 30 mm, both in surgical complications and

Further author information: (Send correspondence to P.P.J.H.L.)
P.P.J.H.L.: E-mail: p.p.j.h.langenhuizen@tue.nl, Telephone: +31 6 83 24 21 60

Medical Imaging 2019: Computer-Aided Diagnosis, edited by Kensaku Mori, Horst K. Hahn, Proc. of SPIE Vol. 10950, 109504C · © 2019 SPIE
CCC code: 1605-7422/19/$18 · doi: 10.1117/12.2512472

in QOL.[4] Moreover, GKRS is generally preferred over microsurgery as it is an outpatient treatment, whereas microsurgery requires hospitalization. Furthermore, microsurgery is more expensive[5] and more invasive for the patient, with a higher risk of hearing loss,[2] facial neuropathy,[6] and other morbidities.

Despite these major advantages over microsurgery, GKRS has one significant drawback: in some cases the intended treatment goal of stopping tumor growth is not achieved, as the tumors display recurring or continuing growth after treatment. This drawback requires lifelong surveillance and even salvage treatment, provided that recurrence is determined. *A-priori* prediction of the treatment response can help in selecting the best treatment modality on an individual basis. Several approaches to this challenge have already been explored.

A first approach is to exploit clinical factors for deriving a predictive value, such as the size of the tumor at treatment[7] and the pre-treatment growth rate.[8] It has been shown that these factors yield some correlation to the treatment outcome. A second approach involves the analyses of MRI characteristics, such as texture quantification[9] and cystic tumor classification,[10] which have also displayed prognostic correlations.

However, the influence of the GKRS treatment procedure itself on the outcome has not been investigated extensively. Publications exploring the effect of the treatment planning limit their investigation to global parameters, such as the prescribed dose to the tumor, the number of radiation shots, and the beam-on time. In a systematic review by Germano *et al.*, the authors conclude that within the range of doses used for the treatment of VS, a lower dose had little to no appreciable difference in progression-free survival, while generally high rates of progression-free survival were reported across a wide range of delivered doses.[11] Treatment with the Gamma Knife is thought to be very uniformly planned, conform protocols, similar to that of other radiosurgical modalities, such as CyberKnife or linear accelerator (LINAC). However, when comparing GKRS to these other modalities, it is determined to be significantly less homogeneous for an elliptical target.[12] This is not unexpected, as GKRS employs a widely varying number of radiation shots with varying shapes, sizes, and weights, in contrast to for example LINAC, which uses only a single shot. Moreover, in a publication by Millar *et al.*,[13] the authors determined that the biological effectiveness of a given physical prescription dose fluctuates with these variations in treatment parameters between different patients. However, it remains unclear if the actual differences in biological effectiveness influences the treatment outcomes. Nevertheless, it is hypothesized that the inhomogeneous dose distribution of GKRS could influence the treatment results. However, the inhomogeneity of the dose distribution cannot be expressed in the global parameters commonly employed in literature. This motivates why, in this paper, we explore the predictive value of the dose distribution on the treatment outcome of GKRS on VS. If successful, this research can provide a basis for identifying the most efficient way of treating a VS with GKRS and the option to personalize the treatment, depending on the tumor characteristics, to ultimately increase the success rate of this treatment for VS patients.

This research contributes in a few ways. First and to the best of our knowledge, this paper provides the first experiments into analyzing the impact of the inhomogeneity of the GKRS dose distribution on the treatment outcome for VS tumors. Second, we explore a novel approach to incorporate the spatial information from three-dimensional histogram of oriented gradients (3D-HOG) features of the inhomogeneous dose distribution. For this purpose, we have implemented 3D-HOG to describe these features.

2. METHODS

The steps for realizing the proposed approach are shown in Fig. 1. First, a description of the pre-processing steps applied to the data is provided. Next, the methods for extracting dose-distribution features are presented. These methods are described in more detail below. The final step of the approach consists of classification and prediction of the treatment outcome. Classification is performed by support vector machine (SVM) and validation of these steps is realized with leave-one-out (LOO) and 10-fold cross-validation methods. The performance of classification is measured as accuracy (ACC), true positive rate (TPR), true negative rate (TNR) and area under the receiver operating characteristic curve (AUC). The various processing steps depicted in Fig. 1 jointly form a data analysis algorithm to predict the treatment outcome based on the dose-distribution features.

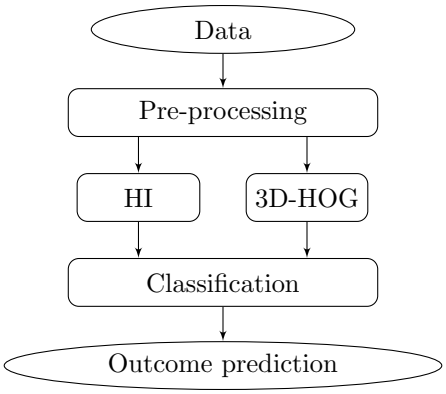

Figure 1. Overview of the processing steps of the prediction algorithm.

2.1 Pre-Processing

For each treatment planning, the neurosurgeon employs a T1-weighted, contrast-enhanced magnetic resonance imaging (MRI) scan. This scan is captured on the day of treatment and is used for segmenting the tumor. This segmentation is required for calculating the quality of the treatment planning in terms of coverage, selectivity and gradient indices. An example of such an MRI scan, including tumor segmentation, is visualized in Part A of Fig. 2. The segmentation points created by the treatment planning software are a set of x- and y-coordinates per MRI slice in the axial MRI plane and are generated with sub-pixel accuracy.

After treatment planning, the dose distribution details are calculated on a $0.5 \times 0.5 \times 0.5$ millimeter grid, representing the stereotactic coordinate system of the Gamma Knife treatment machine. An example of such a dose distribution can be seen in Fig. 2, Part B. In this image, the pixel intensity values are related the dose intensities. Compared to the fine grid of the dose distribution, the segmented tumor contours have a coarse axial resolution. Hence, in order to determine the dose distribution within the tumor, the segmentation contours need to be mapped to the dose distribution space. To achieve this, the following pre-processing steps have been employed. First, both spaces are mapped to the same image coordinate system. Next, a 3D tumor shape is created, using the MATLAB alphaShape tool, by interpolating the contours to fit the axial resolution of the dose distribution. An example of a 3D tumor shape is presented in Fig. 3. The alpha parameter used by the MATLAB tool is minimized per tumor, such that the generated tumor surface does not contain any holes.

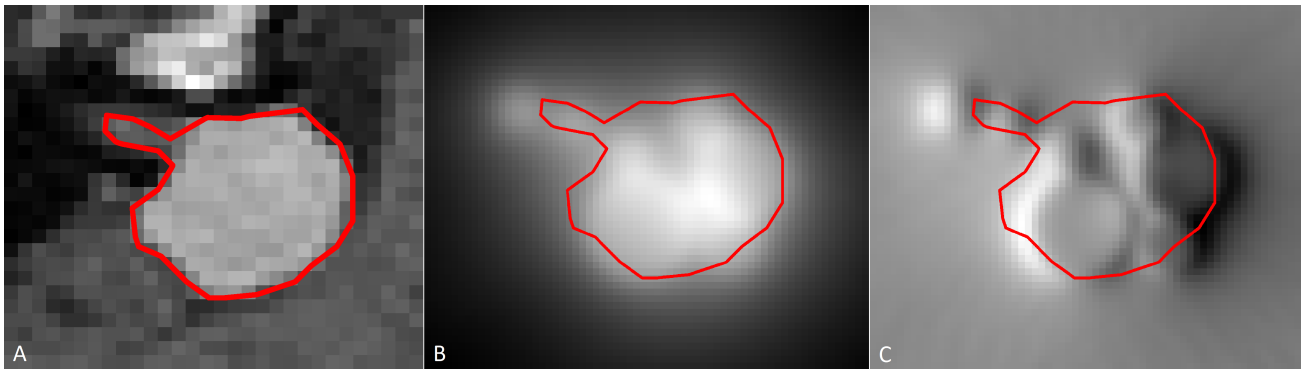

Figure 2. Image examples of the data. The contouring determined by the neurosurgeon during treatment planning is superimposed in red. (A) T1-weighted, contrast-enhanced MRI of a vestibular schwannoma, where the image part containing the tumor is delineated. (B) Calculated dose distribution, where the dose intensities are proportional to the gray-level intensities. (C) Gradient of the dose distribution in the x-direction. The strength of the gradient is represented by the gray-level intensities, where fully white is a strong positive gradient and fully black a strong negative gradient. The different radiation shots used in a GKRS treatment are clearly visible in this image.

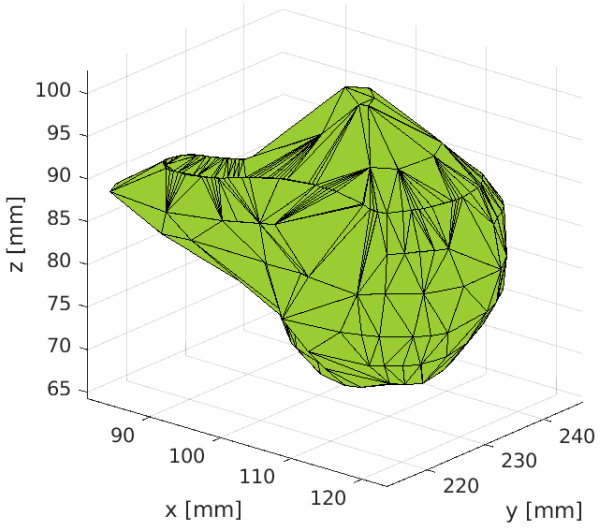

Figure 3. Example of a three-dimensional interpolation of VS contours.

In the final step, the dose distribution voxels inside the interpolated tumor volume are extracted.

2.2 HI Feature Extraction

In order to measure the homogeneity of a dose distribution, Kataria *et al.*[14] have proposed four equations, calculating the homogeneity indices (HIs). The HIs are based on the dose-volume histograms (DVHs). These DVHs are calculated for each patient on the basis of the input percentage. Employing these computations, the following four HI values are calculated by the respective parameters HI_i and the $DVH(x)$:

$$HI_1 = \frac{DVH(5)}{DVH(95)},$$
$$HI_2 = \frac{DVH(1) - DVH(98)}{D_p} \cdot 100\%,$$
$$HI_3 = \frac{DVH(5) - DVH(95)}{D_p} \cdot 100\%,$$
$$HI_4 = \frac{DVH(1)}{D_p}.$$

In the above equations, $DVH(x)$ denotes the minimum dose that $x\%$ of the target volume receives, and D_p is the prescribed dose to the target.

2.3 3D Histogram of oriented gradients

Yu *et al.*[12] determined that GKRS has a highly heterogeneous dose distribution compared to other modalities, due to the calculation of specific HI values. However, these metrics do not consider spatial information. To this end, a three-dimensional histogram of oriented gradients (3D-HOG) is determined on each of the dose distributions, based on the work by Dalal and Triggs in 2D.[15] This is done by calculating the gradients of the dose distribution in x-, y- and z-directions and performing orientation binning. The gradients are computed by employing centered one-dimensional point-derivative masks inside a bounding box of $80 \times 80 \times 64$ voxels. An example of such a gradient of the dose distribution can be found in Part C of Fig. 2. In this image, the heterogeneous character of the dose distribution is clearly visible. Orientation binning is performed in cells, where each cell contains $16 \times 16 \times 16$ voxels, resulting in $5 \times 5 \times 4$ cells for each tumor. Each bin can be interpreted as a unit vector $\vec{b_n}$ in the dose-distribution space with coordinate system (x, y, z). We have used two settings

for the number of bins (vectors), i.e. 6 and 26, resulting in 600 and 2,600 bins (ultimately used as features), respectively. When using 6 bins, every bin (vector) is oriented along an axis in the 3D dose-distribution space in either the positive or negative direction. When employing 26 bins, the additional 20 bins are constructed from the base 6 bins with a separation angle of 45°. Every voxel in a cell invokes the calculation of a gradient, located at that voxel position. This gradient vector $\vec{a}$ is defined by:

$$\vec{a}\,(\vec{x}) = \begin{bmatrix} \partial\vec{x}/\partial x \\ \partial\vec{x}/\partial y \\ \partial\vec{x}/\partial z \end{bmatrix}.$$

Next, the angle θ_n between $\vec{a}$ and every bin $\vec{b_n}$ is computed by determining the angle in a 2D plane between the two vectors. In the 2D case presented in the paper by Dalal and Triggs,[15] every pixel votes for the two closest bins, i.e. the two bins associated with the smallest angle to $\vec{a}$. Here, we employ a 3D-HOG, thus each voxel should vote for three bins. These votes are calculated by:

$$v_k = |\vec{a}|\,\frac{\theta_l + \theta_m}{2\,(\theta_k + \theta_l + \theta_m)}, \tag{1}$$

$$v_l = |\vec{a}|\,\frac{\theta_k + \theta_m}{2\,(\theta_k + \theta_l + \theta_m)}, \tag{2}$$

$$v_m = |\vec{a}|\,\frac{\theta_k + \theta_l}{2\,(\theta_k + \theta_l + \theta_m)}, \tag{3}$$

where k,l and m are the indices of the bins with the smallest angle θ to $\vec{a}$. For each bin within a cell of $16\times16\times16$ voxels, the sum of all its voxel votes is calculated. Subsequently, each cell is represented with an array containing the values of its bins and each dose distribution with an array containing the values for each cell.

3. RESULTS

First, the data used in this research are described, after which the classification results of the individual features are presented. All implementations are realized in MATLAB (MathWorks inc. Natick, Massachusetts, USA). Training of the models is performed by the Classification Learner Application in MATLAB using default settings. For the 3D-HOG features, principal component analysis (PCA) is applied to limit the number of features by using the most relevant Eigenvalues and discarding the other ones.

3.1 Dataset

The dataset in this research involved clinical dose distribution data of 40 selected VS tumors. The VS segmentation contours were drawn by the neurosurgeon during treatment planning, and are thus available for each tumor while the volumetric response to GKRS is also known. The treatment resulted in a failure on 20 tumors, and on the remaining 20 tumors GKRS was successful. Treatment outcome was determined by evaluating the volumetric response, where an increase in tumor volume is considered a failure. This evaluation was performed in a clinical setting by a medical team of specialists. In contrast to this, treatment success is difficult to define. The response of VS to GKRS can only be determined after years of follow-up, where treatment failures can still occur after several years.[8] To this end, we selected tumors that displayed a significant decrease in volume within a relative short time-period following treatment. The relative tumor volumes are plotted over time in Fig. 4, where time was defined at treatment moments and at follow-up visits. The dose distribution is calculated by the treatment planning software (GammaPlan, Elekta AB, Stockholm, Sweden) and is mapped to a 3D space with a resolution of $0.5\,\text{mm}\times0.5\,\text{mm}\times0.5\,\text{mm}$, with every element containing a high-precision representation (16 bits) of the delivered dose.

3.2 Homogeneity indices

Employing the DVH per tumor, the HI features and their mean and variance for the two patient cohorts are calculated. The resulting statistics are depicted in Table 1. To evaluate the differences between the two cohorts, the results for each HI are tested using a paired t-test. The resulting p-values are also depicted in Table 1. There

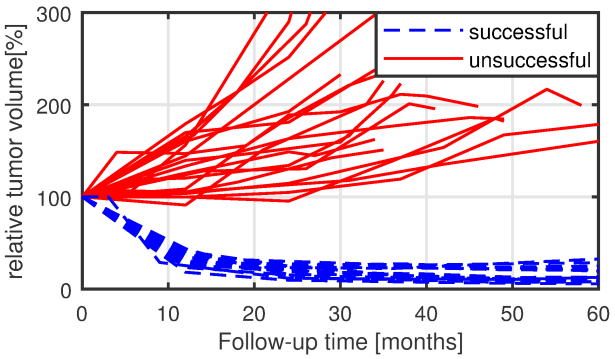

Figure 4. Volumetric response of the 20 successfully (blue) and 20 unsuccessfully (red) treated VS tumors. In this graph, follow-up time equal to 0 represents the treatment time. Response is given as a volume ratio with respect to the tumor volume at time of treatment.

Table 1. Statistical description of the resulting HI values. For each HI feature, the mean and standard deviation (std.) are presented, including the resulting p-values from the paired t-tests comparing the two cohorts.

	Successful		**Unsuccessful**		
	Mean	**Std.**	**Mean**	**Std.**	**p-value**
HI_1	1.94	0.72	1.80	0.27	0.39
HI_2	97.8	31.4	93.6	27.1	0.59
HI_3	73.2	26.6	69.7	19.5	0.59
HI_4	1.80	0.28	1.77	0.25	0.61

is no significant statistical difference between the two cohorts, as indicated by a p-value smaller than 0.05. Thus, it can be concluded that there is no statistical difference in HI values between the successfully treated tumors and the tumors for which treatment failed. Indeed, employing these features in a machine learning algorithm did not obtain good results (see Table 2). The highest-performing SVM trained on these features obtained an ACC of 52.5%, showing that these features cannot distinguish treatment failure from treatment success.

3.3 3D Histogram of oriented gradients

Employing a bounding box of $80 \times 80 \times 64$ voxels, divided into $5 \times 5 \times 4$ cells, we obtain a number of 3D-HOG features equal to 100 times the number of bins. Since this number of features is high, PCA is employed to reduce this number. The classification results of these 3D-HOG features show that overall, linear SVM obtained the highest ACC values, regardless of the amount of principal components or bins. The highest ACC (77.5%) was obtained by employing 26 bins, 20 principal components and 10-fold cross-validation. The resulting TPR, TNR and AUC are 80%, 75% and 0.79, respectively. Results of the other SVMs obtained by employing 26 bins and 20 principal components are presented in Table 3. The SVMs obtained by employing 6 bins show similar results.

4. DISCUSSION

This study was designed to investigate the possible influence of the GKRS dose distribution on the treatment response for vestibular schwannoma. For the binary classification problem in this research, treatment success and treatment failure need to be defined. The objective of a GKRS treatment on vestibular schwannoma is to stop tumor expansion. From this objective, it is easy to define treatment failure. However, continuous or even recurring tumor growth can occur as late as 10 years following treatment. As such, treatment success is not simply 'no failure', even after several years of follow-up. To this end, we have selected tumors that showed a significant volume reduction in the first year following GKRS. This definition of treatment success has enabled us to create two very dissimilar cohorts of each 20 patients, so that the experiment was technically well-defined. However, this definition causes a limitation on the actual evaluation of the dose-distribution influence, as it

Table 2. Classification performance for homogeneity indices, measured in accuracy (ACC), true positive rate (TPR), true negative rate (TNR), and area under the ROC curve (AUC). Results are obtained from six support vector machine (SVM) models. Validation was performed by 10-fold cross-validation and leave-one-out (LOO) cross-validation.

SVM Type	Validation	ACC(%)	TPR(%)	TNR(%)	AUC
Linear	10-fold	40.0	70	10	0.32
	LOO	12.5	5	20	0.05
Quadratic	10-fold	52.5	55	50	0.53
	LOO	37.5	40	35	0.41
Cubic	10-fold	52.5	55	50	0.40
	LOO	40	40	40	0.28
Fine Gaussian	10-fold	50	50	50	0.59
	LOO	42.5	40	45	0.51
Medium Gaussian	10-fold	45	40	50	0.38
	LOO	17.5	5	30	0.03
Coarse Gaussian	10-fold	45	5	85	0.39
	LOO	0	0	0	0

Table 3. Classification performance for 3D-HOG features with 10-fold cross-validation, measured in accuracy (ACC), true positive rate (TPR), true negative rate (TNR), and area under the ROC curve (AUC). Results are obtained from six support vector machine (SVM) models. Validation was performed by 10-fold cross-validation and leave-one-out (LOO) cross-validation. The bold-font numbers indicate the highest scores.

SVM Type	Validation	ACC(%)	TPR(%)	TNR(%)	AUC
Linear	10-fold	**77.5**	**80**	**75**	**0.79**
	LOO	72.5	75	70	0.75
Quadratic	10-fold	67.5	75	60	0.77
	LOO	67.5	70	65	0.71
Cubic	10-fold	62.5	75	50	0.79
	LOO	65	75	55	0.73
Fine Gaussian	10-fold	55	45	65	0.59
	LOO	0	0	0	0
Medium Gaussian	10-fold	65	75	55	0.77
	LOO	62.5	75	50	0.72
Coarse Gaussian	10-fold	75	75	75	0.77
	LOO	0	0	0	0

provides a bias in the data. Hence, the influence of the dose distribution needs to be investigated further on larger datasets, with a broader definition of treatment success. Previous work shows no influence of general dose parameters on the treatment outcome. However, the obtained results found in this research, with our definitions of failure and success, suggest that the dose distribution does correlate to the treatment outcome (AUC = 0.79, TPR = 80%, TNR = 75%, with linear SVM).

5. CONCLUSIONS

At present, it remains undetermined what affects the GKRS treatment outcome on vestibular schwannoma. Research on this topic has revealed some correlation of clinical factors, such as tumor volume and growth rate. Furthermore, MRI characteristics such as first-order statistics and features based on gray-level co-occurrence and run-length matrices have shown correlation to the GKRS treatment outcome. However, the GKRS treatment planning itself has not been investigated thoroughly. Inherently, GKRS treatments are highly heterogeneous in dose distribution and this could potentially influence the efficacy of the treatment. This research contributes in three ways. First and to the best of our knowledge, this paper provides the first experiments into analyzing

the impact of the inhomogeneity of the GKRS dose distribution on the treatment outcome for VS tumors. Second, besides implementing a previously employed method for determining differences in dose distributions by Kataria *et al.*, we have explored a novel approach to incorporate the spatial information from 3D-HOG features of the inhomogeneous dose distribution. We have implemented 3D-HOG to describe these differences. Third, we have found that the correlation of homogeneity indices with the treatment outcome in our dataset presented no statistical evidence of an association, whereas the 3D-HOG features do present correlations to the treatment outcome (AUC = 0.79, TPR = 80%, TNR = 75%, with linear SVM). The details in the 3D-HOG features suggest that, even though treatment planning is considered uniform, there are measureable differences that could potentially influence the treatment efficacy. These findings can provide a basis for refining towards personalized treatments and prediction of treatment efficiency. However, these results need to be more extensively analyzed on larger datasets.

REFERENCES

[1] Olson, J. J., Kalkanis, S. N., and Ryken, T. C., "Congress of Neurological Surgeons Systematic Review and Evidence-Based Guidelines on the Treatment of Adults with Vestibular Schwannomas: Executive Summary," in [*Clinical Neurosurgery*], **82**, 129–134 (feb 2018).

[2] Soulier, G., van Leeuwen, B. M., Putter, H., Jansen, J. C., Malessy, M. J., van Benthem, P. P. G., van der Mey, A. G., and Stiggelbout, A. M., "Quality of Life in 807 Patients with Vestibular Schwannoma: Comparing Treatment Modalities," *Otolaryngology - Head and Neck Surgery (United States)* **157**(1), 92–98 (2017).

[3] Kondziolka, D., Mousavi, S. H., Kano, H., Flickinger, J. C., and Lunsford, L. D., "The newly diagnosed vestibular schwannoma: radiosurgery, resection, or observation?," *Neurosurgical Focus* **33**(3), E8 (2012).

[4] Wolbers, J. G., Dallenga, A. H., Mendez Romero, A., and van Linge, A., "What intervention is best practice for vestibular schwannomas? A systematic review of controlled studies.," *BMJ open* **3** (1 2013).

[5] Caruso, J. P., Moosa, S., Fezeu, F., Ramesh, A., and Sheehan, J. P., "A cost comparative study of Gamma Knife radiosurgery versus open surgery for intracranial pathology," *Journal of Clinical Neuroscience* **22**, 184–188 (1 2015).

[6] Arthurs, B. J., Fairbanks, R. K., Demakas, J. J., Lamoreaux, W. T., Giddings, N. A., Mackay, A. R., Cooke, B. S., Elaimy, A. L., and Lee, C. M., "A review of treatment modalities for vestibular schwannoma," *Neurosurgical Review* **34**, 265–279 (7 2011).

[7] Klijn, S., Verheul, J. B., Beute, G. N., Leenstra, S., Mulder, J. J. S., Kunst, H. P. M., and Hanssens, P. E. J., "Gamma Knife radiosurgery for vestibular schwannomas: evaluation of tumor control and its predictors in a large patient cohort in The Netherlands," *Journal of Neurosurgery* **124**, 1619–1626 (6 2016).

[8] Langenhuizen, P. P. J. H., Zinger, S., Hanssens, P. E. J., Kunst, H. P. M., Mulder, J. J. S., Leenstra, S., de With, P. H. N., and Verheul, J. B., "Influence of pretreatment growth rate on Gamma Knife treatment response for vestibular schwannoma: a volumetric analysis," *Journal of Neurosurgery* **-1**, 1–8 (nov 2018).

[9] Langenhuizen, P., Legters, M., Zinger, S., Verheul, J., de With, P. N., and Leenstra, S., "MRI textures as outcome predictor for Gamma Knife radiosurgery on vestibular schwannoma," in [*Medical Imaging 2018: Computer-Aided Diagnosis*], Mori, K. and Petrick, N., eds., 16, SPIE (2 2018).

[10] Frisch, C., Jacob, J., Carlson, M., Driscoll, C., Neff, B., and Link, M., "Stereotactic Radiosurgery for Cystic Vestibular Schwannomas," *Journal of Neurological Surgery Part B: Skull Base* **76**, A116 (2 2015).

[11] Germano, I. M., Sheehan, J., Parish, J., Atkins, T., Asher, A., Hadjipanayis, C. G., Burri, S. H., Green, S., and Olson, J. J., "Congress of Neurological Surgeons Systematic Review and Evidence-Based Guidelines on the Role of Radiosurgery and Radiation Therapy in the Management of Patients With Vestibular Schwannomas," *Neurosurgery* **82**, E49–E51 (feb 2018).

[12] Yu, C., Jozsef, G., Apuzzo, M. L., and Petrovich, Z., "Dosimetric Comparison of CyberKnife with Other Radiosurgical Modalities for an Ellipsoidal Target," *Neurosurgery* **53**, 1155–1163 (11 2003).

[13] Millar, W. T., Hopewell, J. W., Paddick, I., Lindquist, C., Håkan Nordström, H., Lidberg, P., and Gårding, J., "The role of the concept of biologically effective dose (BED) in treatment planning in radiosurgery," *Physica Medica* **31**, 627–633 (9 2015).

[14] Kataria, T., Sharma, K., Subramani, V., Karrthick, K. P., and Bisht, S. S., "Homogeneity Index: An objective tool for assessment of conformal radiation treatments.," *Journal of medical physics* **37**, 207–213 (10 2012).

[15] Dalal, N. and Triggs, W., "Histograms of Oriented Gradients for Human Detection," *2005 IEEE Computer Society Conference on Computer Vision and Pattern Recognition CVPR05* **1**(3), 886–893 (2005).